Chang, J.-Y., Ngai, P., Rink, H., Dennis, S., & Schläppi, J. M. (1990) *FEBS Lett. 261*, 287-290.
Dennis, S., Wallace, A., Hofsteenge, J., & Stone, S. R. (1990) *Eur. J. Biochem. 188*, 61-66.
Dodt, J., Schmitz, T., Schäfer, T., & Bergmann, C. (1986) *FEBS Lett. 202*, 373-377.
Dodt, J., Köhler, S., Schmitz, T., & Wilhelm, B. (1990) *J. Biol. Chem. 265*, 713-714.
Fenton, J. W., III (1981) *Ann. N.Y. Acad. Sci. 370*, 468-495.
Fenton, J. W., II, Landis, B. H., Walz, D. A., & Finlayson, J. S. (1977a) in *Chemistry and Biology of Thrombin* (Lundblad, R. L., Fenton, J. W., II, & Mann, K. G., Eds.) pp 43-70, Ann Arbor Science Publishers, Ann Arbor, MI.
Fenton, J. W., II, Fasco, M. J., Stackrow, A. B., Aronson, D. L., Young, A. M., & Finlayson, J. S. (1977b) *J. Biol. Chem. 252*, 3587-3598.
Grütter, M. G., Priestle, J. P., Rahuel, J., Grossenbacher, H., Bode, W., Hofsteenge, J., & Stone, S. R. (1990) *EMBO J. 9*, 2361-2365.
Hofsteenge, J., Taguchi, H., & Stone, S. R. (1986) *Biochem. J. 237*, 243-251.
Hofsteenge, J., Braun, P. J., & Stone, S. R. (1988) *Biochemistry 27*, 2144-2151.
Jameson, G. W., Roberts, D. V., Adams, R. W., Kyle, W. S. A., & Elmore, D. T. (1973) *Biochem. J. 131*, 101-117.
Laidler, K. J. (1987) *Chemical Kinetics*, pp 191-202, Harper and Row, New York.
Lewis, S. D., Lorand, L., Fenton, J. W., II, & Shafer, J. A. (1987) *Biochemistry 26*, 7597-7603.
Lottenberg, R., Hall, J. A., Fenton, J. W., II, & Jackson, C. M. (1982) *Thromb. Res. 28*, 313-332.
Morrison, J. F. (1982) *Trends Biochem. Sci. 7*, 102-105.
Noë, G., Hofsteenge, J., Rovelli, G., & Stone, S. R. (1988) *J. Biol. Chem. 263*, 11729-11735.
Riehl-Bellon, N., Carvallo, D., Acker, M., Van Dorsselaer, A., Marquet, M., Loison, G., Lemoine, Y., Brown, S. W., Courtney, M., & Roitsch, C. (1989) *Biochemistry 28*, 2941-2949.
Rydel, T. J., Ravichrandran, K. G., Tullinsky, R., Bode, W., Huber, R., Roitsch, C., & Fenton, J. W., II (1990) *Science 245*, 277-280.
Segal, I. H. (1975) *Enzyme Kinetics*, pp 196-198, Wiley, New York.
Sonder, S. A., & Fenton, J. W., II (1986) *Clin. Chem. (Winston-Salem, N.C.) 32*, 934-937.
Stone, S. R., & Hofsteenge, J. (1986) *Biochemistry 25*, 4622-4628.
Stone, S. R., Braun, P. J., & Hofsteenge, J. (1987) *Biochemistry 26*, 4617-4624.
Stone, S. R., Dennis, S., & Hofsteenge, J. (1989) *Biochemistry 28*, 6857-6863.
Wallace, A., Dennis, S., Hofsteenge, J., & Stone, S. R. (1989) *Biochemistry 28*, 10079-10084.

Deuterium Quadrupole Coupling in *N*-Acetylglycine and Librational Dynamics in Solid Poly(γ-benzyl-L-glutamate)†

M. G. Usha,‡ W. L. Peticolas,§ and R. J. Wittebort*,‡
Department of Chemistry, University of Louisville, Louisville, Kentucky 40292, and Department of Chemistry, University of Oregon, Eugene, Oregon 97403

Received September 19, 1990; Revised Manuscript Received December 17, 1990

ABSTRACT: To study the dynamics of peptide groups in solid proteins, we have accurately determined the principal components and molecular orientation of the electric field gradient tensor for the exchangeable deuterons in monoclinic *N*-acetylglycine by single-crystal deuterium nuclear magnetic resonance. These results are compared with the principal components of the amide deuterons in solid poly(γ-benzyl-L-glutamate) measured in powder samples over a wide temperature range (140-400 K). The comparison indicates that in the solid polypeptide the N-D bonds undergo a small-amplitude torsional reorientation (libration) perpendicular to the peptide plane. To estimate dynamic rates, longitudinal relaxation times (T_1 values) are reported for *N*-acetylglycine and poly(γ-benzyl-L-glutamate). T_1 values for the carboxyl and amide deuterons in *N*-acetylglycine are $\sim$100 s, whereas for the amide deuterons in the polypeptide $T_1 \sim 1$ s, also indicating that the N-D bonds are not stationary in the polypeptide. We determine from the reduced quadrupole coupling tensor the mean-square amplitude for the libration and show that it increases linearly with temperature. A simple qualitative theory for the relaxation times is presented on the basis of the assumption that the N-D reorientation is described either as a diffusion process in a square well or as a damped Langevin oscillator with a harmonic restoring force. The conclusion is that the short relaxation times of the polypeptide amide deuterons result from substantial frictional effects on reorientation that increase with temperature.

We have used deuterium magnetic resonance to study monoclinic crystals of amide- and carboxyl-deuterated *N*-acetylglycine (NAG)[1] and amide-deuterated polycrystalline poly(γ-benzyl-L-glutamate) (PBG). Once the quadrupole coupling or electric field gradient (efg) tensor principal components and molecular orientation are known for the amide

† This work was supported by grants from the National Science Foundation (DMB8918376 to R.J.W.) and the National Institutes of Health (GM 15547-24 to W.L.P.).
* Author to whom correspondence should be addressed.
‡ Department of Chemistry, University of Louisville.
§ Department of Chemistry, University of Oregon.

[1] Abbreviations: efg, electric field gradient tensor; T_1, longitudinal relaxation time; NAG, *N*-acetylglycine; PBG, poly(γ-benzyl-L-glutamate).

0006-2960/91/0430-3955$02.50/0

deuteron of a reasonable peptide analogue such as NAG, the rate and amplitude of backbone librational dynamics in solid polypeptides such as PBG can be examined by ^2H NMR. The efg tensor for amide deuterons is typically nonaxial, thus the three principal components conveniently frequency label the three axes of an orthogonal coordinate system attached to the N–D bond. Dynamic averaging of these components as monitored by the ^2H NMR experiment allows one to determine to what extent reorientation about each of the orthogonal axes occurs.

The structure of *N*-acetylglycine has been determined by both X-ray and neutron diffraction (Donohue & Marsh, 1962; Mackay, 1975) both of which show a highly ordered molecule devoid of solid-state molecular dynamics aside from a rotating methyl group. Thus we use single-crystal and powder ^2H NMR spectra of this material to establish the principal values and molecular orientation of the amide- and carboxyl-deuteron electric field gradient tensors and the deuteron relaxation times, T_1, in a rigid system. We present a simple procedure for using the crystallographic symmetry to accurately determine the molecular orientation of the deuteron electric field gradient tensors (Experimental Procedures) and discuss the advantage of comparing the ^2H NMR results with the neutron structure rather than the X-ray structure. The quadrupole coupling constants determined here are successfully compared with empirical relations based on hydrogen-bond lengths. These results are useful for deuterium magnetic resonance studies of molecular ordering and dynamics of polypeptides in any anisotropic phase such as solid polymers, liquid crystals (Poliks et al., 1987), or crystalline (Usha & Wittebort, 1989) and fibrous proteins (Chapman et al., 1970). Previously, such studies have relied on the electric field gradient tensor of urea-d_4 (Chiba, 1965), which is not a good chemical analogue of the peptide group.

The temperature dependence of the principal components of the efg tensor and the longitudinal relaxation times are reported for the amide deuterons of PBG. Both indicate the presence of small-amplitude torsional dynamics that are discussed in detail. A simple expression is presented that allows for the direct evaluation of a mean-square librational amplitude from the residual quadrupole coupling components measured from a ^2H NMR powder pattern. The linear temperature dependence of the mean-square amplitude suggests harmonically bound oscillatory motion, and on the basis of simple structural considerations, we estimate an upper limit for the mode frequency. Subsequently, the PBG relaxation times and their temperature dependence are analyzed in terms of small-amplitude diffusive dynamics or damped oscillatory motion based on the Langevin model. The required expressions for relating NMR relaxation times to a diffusion or damping constant and mean-square amplitude or mode frequency are presented in the appendix. Surprisingly, the diffusive and Langevin models in the limit of fast, small-amplitude motion yield nearly equivalent relaxation expressions that when applied to the relaxation data indicate the importance of frictional effects for amide dynamics in PBG.

Experimental Procedures

Materials. L-Pyroglutamic acid and *N*-acetylglycine were obtained from Sigma Chemical Co. NAG was recrystallized by slow evaporation of saturated solutions from 99% D_2O, yielding large single crystals (10–40 mg) as judged by optical microscopy. Anhydrous poly(γ-benzyl-L-glutamate-d_1) was prepared by exchanging the polypeptide in CF_3CO_2D. The sample used in this study was kindly provided by Professor E. T. Samulski.

Deuterium Spectroscopy. Variable temperature ^2H NMR spectra were obtained on a home-built 5.9-T (ν_0 = 38.77 MHz) spectrometer described previously (Wittebort et al., 1986). Spectra were obtained with a two-pulse quadrupole echo sequence with 90° pulse widths of 2.5-μs duration and 35-μs spacing. Longitudinal relaxation times, T_1, were measured by inserting a composite inversion pulse (Tycko et al., 1984) at a variable time, τ, before the echo sequence. Relaxation times were determined by least-squares fitting of powder-pattern intensities, $I(t)$, at a given frequency to the standard function $I(\tau) = I_0[1 - 2A \exp(-\tau/T_1)]$ by using a routine based on the Marquardt algorithm (Press et al., 1986). For the powder-pattern frequencies examined, the assumption of single exponential relaxation was found to be satisfactory.

Single-Crystal Measurements. *N*-Acetylglycine crystallizes in the monoclinic space group $P2_1/c$ with a = 4.85 Å, b = 11.54 Å, c = 14.63 Å, and β = 138°, containing four molecules (Donohue & Marsh, 1962; Mackay, 1975). For convenience we use an orthogonal set of lattice vectors (a,b,c^*) with a and b along the crystallographic a and b axes and c^* perpendicular to the a,b-plane ($c^* = a \times b$).

Crystals prepared as described above are monoclinic plates. Two of the faces have an obtuse angle between the edges essentially equal to β, i.e., 138°. Thus the crystal morphology directly parallels the unit cell as follows: a and b are along the orthogonal edges of a rectangular face and are distinguished from each other such that c^* is orthogonal to b and at an angle of 138° with respect to a. The vector c^* is thus normal to a rectangular face. This assignment was confirmed by the consequences of unit-cell symmetry properties on the NMR spectra as described below.

The desired electric field gradient tensors are determined by rotating crystals about three mutually orthogonal axes, conveniently chosen here to be a, b and c^*. Half the frequency difference between the doublets is used as the observed frequency, $\nu_{obs}^{(i)}$, so as to cancel out chemical shifts, in which case the orientation dependence is

$$\pm\nu_{obs}^{(i)}(\phi) = \frac{1}{2}(\nu_{kk} - \nu_{jj}) \cos 2\phi + \nu_{jk} \sin 2\phi + \frac{1}{2}(\nu_{jj} + \nu_{kk}) \quad (1)$$

where ϕ is the goniometer angle for rotation about the ith axis that is perpendicular to the laboratory magnetic field. For the rotation axes, i = (a, b, or c^*), then j = ($-c^*$, $-a$, or a), and k = (b, c^* or b), with c^*, a, and a along $\mathbf{H}_0$ for ϕ = 0, respectively, for the three rotations. With a standard linear least-squares procedure (Press et al., 1986), eq 1 is fit to the frequencies obtained from the three rotations thus determining ν_{ij}, a symmetric and traceless tensor ($\nu_{ij} = \nu_{ji}$ and $\nu_{xx} + \nu_{yy} + \nu_{zz} = 0$) containing five independent components. The three principal axis components or eigenvalues of ν_{ij}, ν_{ii}^{PAS}, then determine the quadrupolar coupling, e^2qQ/h, and the asymmetry, η, according to

$$e^2qQ/h = \frac{4}{3}\nu_{zz}^{PAS} \quad \text{and} \quad \eta = \frac{\nu_{xx}^{PAS} - \nu_{yy}^{PAS}}{\nu_{zz}^{PAS}} \quad (2)$$

$$\nu_{zz}^{PAS} \geq \nu_{yy}^{PAS} \geq \nu_{xx}^{PAS}$$

The corresponding eigenvectors contain the direction cosines (projections) of the electric field gradient tensor principal axes on the rotation axes, which in this case are the orthogonal unit-cell axes a and b and the normal to the a,b-plane, c^*. Alternatively, the direction cosines can be expressed as three Euler angles (α,β,γ) (Arfken, 1971).

The four molecules per unit cell contain pairs related by a center of inversion and thus are magnetically equivalent since

Table I: Deuterium Electric Field Gradient Tensor Coupling Constants, Asymmetries, and Orientations in *N*-Acetylglycine ($CH_3CONDC^{\alpha}H_2C^{o}O_2D$)[a]

^2H	$\lvert e^2qQ/h\rvert$	η	tensor (α,β,γ)	bond (θ,ϕ)	ν_{yy}^{PAS} (θ,ϕ)	plane (θ,ϕ)
(O–D)	137 (2)	0.121 (5)	93 (3), 47 (3), −7 (3)	47.4, −7.6	43 (3), 177 (3)	43.0, 181.5
(O–D)′	137 (2)	0.121 (5)	93 (3), 133 (3), 187 (3)	132.6, 187.6	43 (3), −177 (3)	43.0, −181.5
(N–D)	210 (2)	0.137 (5)	51 (3), 69 (3), 62 (3)	69.1, 62.4	44 (3), 176 (3)	43.4, 177.0
(N–D)′	210 (2)	0.137 (5)	51 (3), 111 (3), 118 (3)	111.7, 117.6	44 (3), −176 (3)	43.4, −177.0

[a] Euler angles are given in degrees referenced to the (a,b,c^*) system. Planes are defined by the vectors normal to the planes containing the N, D, and C^{α} or the C^{o}, O, and D atoms for the carboxyl or amide deuterons, respectively. Primed and unprimed deuterons of the same chemical type are related by the ac^* mirror plane.

the quadrupole coupling transforms as a second-rank tensor. The magnetically nonequivalent molecules are related by mirror symmetry about the a,c^* plane. Thus for the general orientation we expect the ^2H NMR spectrum to show four doublets, two each from the magnetically nonequivalent amide and carboxyl deuterons. However, for rotation about the b axis, the tensor projections on to $\mathbf{H_0}$ are necessarily equivalent, and the deuterons related by mirror symmetry become magnetically equivalent, reducing the spectrum to two doublets. Thus, for this coordinate system, the lattice symmetry requires that the tensors for two mirror-plane-related deuterons, ν_{ij} and ν_{ij}', have the following properties, $\nu_{ii} = \nu_{ii}'$, $\nu_{ac^*} = \nu_{ac^*}'$, $\nu_{ab} = -\nu_{ab}'$, and $\nu_{bc^*} = -\nu_{bc^*}'$. In the work reported here, the three rotations were performed on three different crystals, and small misalignments can lead to breakdown of the symmetry constraints. We found that within 4 kHz the above relations were always observed experimentally. In practice we thus imposed these symmetry conditions by taking appropriate averages. For each of the diagonal elements, the average was taken over the six values determined for the two symmetry-related deuterons for the three rotations, and for the off-diagonal elements the magnitudes were averaged for the two mirror-related deuterons.

With the orthogonal rotations used here, the mirror-symmetry-related deuterons are equivalent for the a and c^* rotations and the $\phi = 0$ setting, thus introducing an ambiguity as to consistently assigning the rotation curves in all three rotations to a given deuteron. This ambiguity was resolved by forming all possible tensors and comparing their eigenvalues with those determined experimentally from a powder sample. In all four cases, two combinations gave eigenvalues in excellent agreement with the powder values, whereas the other combinations gave substantially different eigenvalues.

Results and Discussion

Room-temperature ^2H NMR spectra of *N*-acetylglycine obtained at selected goniometer settings and rotation about the c^* axis are shown in Figure 1. Spectra were acquired with a quadrupole echo sequence with a delay of 5–10 min between consecutive acquisitions. To obtain full equilibrium signal intensities, delays on the order of 20–30 min are required. The long relaxation time is completely consistent with a rigid molecular structure. From the thermal parameters of the neutron structure (Mackay, 1975), root-mean-square displacements of the amide N and H atoms are less than 0.1 Å. For two of the lines, orientations showing large quadrupolar splittings consistently show substantial broadening. This results from dipolar coupling with abundant ^{14}N and thus distinguishes the amide and carboxyl deuterons. The effect is observed only for lines with large quadrupole splittings since the large components of both the quadrupole and dipole coupling tensors are coaxial, i.e., along the ^{14}N–D bond axis as shown below. Graphs of the doublet frequencies as a function of goniometer angle for rotation about the a and b axes are shown Figure 2. The expected four doublets are observed for the

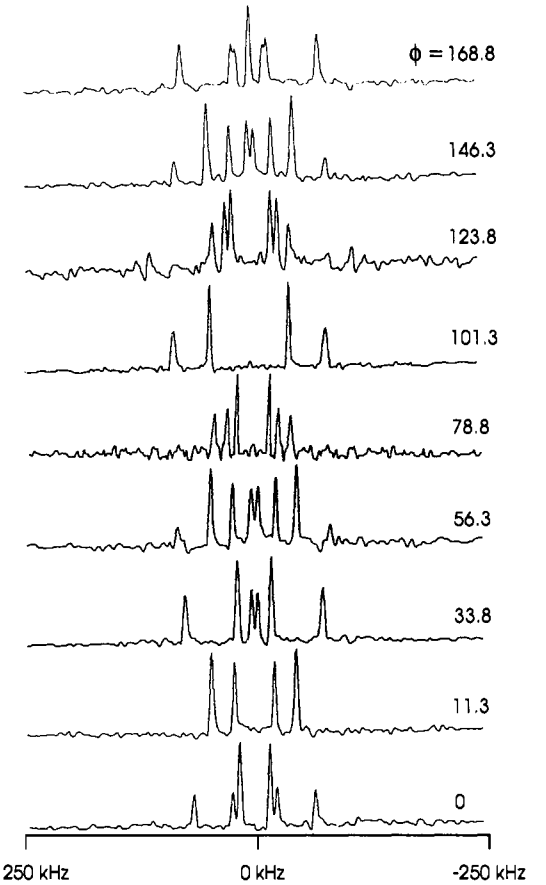

FIGURE 1: ^2H NMR spectra of a single crystal of *N*-acetylglycine shown for selected goniometer settings, ϕ, and rotation about the c^* axis. Each spectrum results from signal averaging of 4–20 transients.

a- and c^*-axis (not shown) rotations, and as expected on the basis of the unit-cell symmetry, the graph is symmetric about $\phi = 90°$. The b-axis rotation, rather than two doublets, shows that one of the expected doublets is slightly split due to a small misalignment of the crystal.

Quadrupole couplings, asymmetries and Euler angles resulting from the analysis of the single-crystal data are listed in Table I. The uncertainty in the Euler angles, ±3°, is our estimation of how precisely the crystals were mounted. Euler angles are referenced to the orthogonal lattice system (a,b,c^*) defined in the previous section. In this system the polar orientation (θ,ϕ) for the largest principal component, ν_{zz}^{PAS}, is just (β,γ), and for convenience the orientation of the y component, ν_{yy}^{PAS}, is also listed. For comparison with the molecular structure, orientations of the N–D or O–D bond axes and the vectors normal to the planes containing the D, N, and C^{α} or the D, O, and C^{o} atoms are given. The tensors are assigned to amide or carboxyl deuterons on the basis of the observation of ^{14}N dipolar broadening of the amide deuteron doublets. The ^2H NMR powder pattern of NAG shows two couplings and asymmetries (error limits in parentheses): e^2qQ/h = 137 (2) kHz and η = 0.12 (1); and e^2qQ/h = 211 (2) kHz and η =

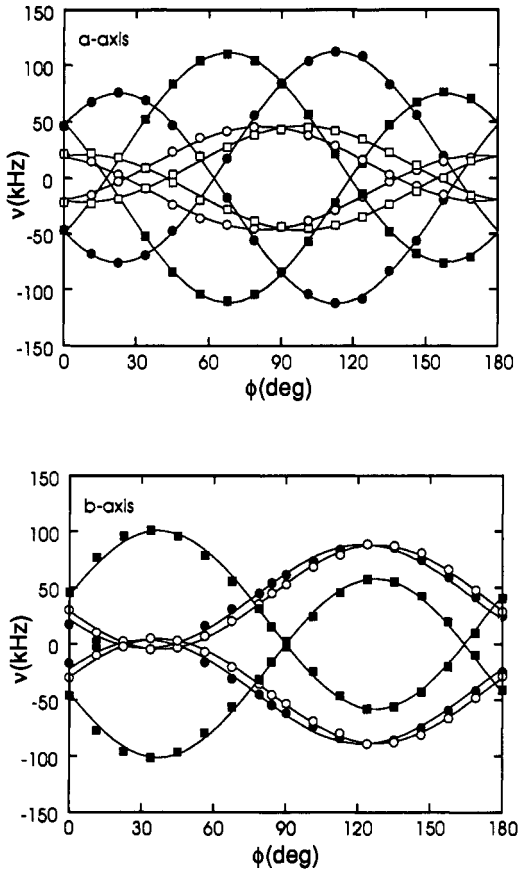

FIGURE 2: Graphs of the ^2H NMR doublet frequencies for the *a*- and *b*-axis rotations.

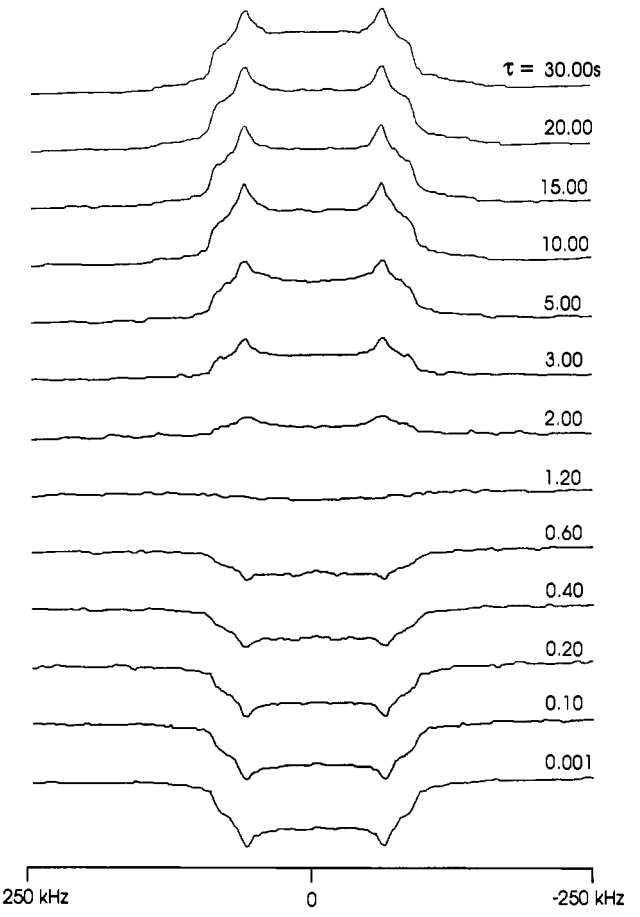

FIGURE 3: Inversion–recovery spectra of poly(γ-benzyl-L-glutamate) obtained at 289 K. The indicated time, τ, on each spectrum is the delay between the inversion and observe pulse sequences.

0.13 (1), in excellent agreement with the values obtained from single crystals. Assignments of the two observed tensor orientations to the chemically equivalent deuterons related by the *a*,*c** mirror plane conform with the usual expectation that the largest principal component is directed approximately along the bond axis. With these assignments, the largest principal components, ν_{zz}^{PAS}, for both the carboxyl and amide deuterons lie well within experimental error along the bond axes, and the components of intermediate magnitude, ν_{yy}^{PAS}, are normal to the D–N–C$^\alpha$ or D–O–C° planes. The neutron structure shows the N–D bond axis about 2° out of the usual peptide plane, and this plane, although conveniently defined in terms of the molecular structure, is thus not a precise reference for the orthogonal tensor components. From Table I it is seen that the principal axis systems for the carboxyl and amide deuterons are conveniently related to the molecular structure by the deuterium bond vector and the normal to the D–N–C$^\alpha$ or D–O–C° planes, respectively. The largest component of the electric field gradient tensor lies along the bond vector, the component of intermediate magnitude is normal to the molecular plane, and the smallest component is along the axis mutually orthogonal to the bond vector and molecular plane. Although the amide group is chemically distinct from an amino group, the amide deuteron electric field gradient tensor orientation determined here for NAG is essentially equivalent to that for amine deuterons in urea (Chiba, 1965). It thus appears that this efg tensor orientation is transferable to a variety of chemically related systems.

Simple empirical relations of the form

$$e^2qQ/h = A - Br^{-3} \quad (3)$$

have been proposed that relate quadrupole couplings to covalent- or hydrogen-bond lengths, *r*. For N–D···O systems the constants are $A = 282$ and $B = -572$ (Hunt & Mackay, 1976) with *r* in Å and e^2qQ/h in kHz. The neutron structure for NAG shows the amide deuteron intermolecularly hydrogen bonded to the glycyl carbonyl oxygen at a distance of 2.16 Å, from which we calculate a coupling of 225 kHz or about 7% larger than the measured value, 210 (2) kHz. For O–D···O systems the constants are $A = 328$ and $B = 643$, where *r* is the D···O distance (Hunt & Mackay, 1976), or alternatively $A = -327$ and $B = 533$, where *r* is the O–D length (Looyestijn et al., 1979). The carboxyl deuteron has hydrogen-bond and covalent distances of 1.514 and 1.034 Å, respectively, from which we calculate couplings of 143 or 155 kHz. The value calculated on the basis of the hydrogen-bond distance is 4% larger than the observed value, 137 (2) kHz. The agreement between experiment and empirical relations for both deuteron types is well within the scatter associated with the empirical expressions and indicates that the couplings observed in this work are not unusual. For additional comparison we have measured the amide deuteron coupling and asymmetry for another simple amide deuteron, L-pyroglutamic acid, in which the side-chain γ-carboxyl forms an intermolecular amide linkage with the α-amino group. The X-ray structure (Van Zoeren et al., 1978) shows the amide group intermolecularly hydrogen bonded to a carbonyl oxygen with an H–O distance of 2.3 Å. The deuterium spectrum has a long relaxation time of more than a minute and $e^2qQ/h = 209$ (2) kHz, in good agreement with the value measured for NAG. The asymmetry, $\eta = 0.13$ (1), is somewhat smaller than that for PBG but the same as for NAG.

We now consider the results of ^2H NMR studies of polycrystalline PBG. Shown in Figure 3 are a series of inversion–recovery powder spectra obtained from amide-deuterated

Table II: ^2H NMR Longitudinal Relaxation Times (s) for the Amide Deuterons in Polycrystalline PBG for the Indicated Powder Pattern Frequencies and Temperatures

T (K)	T_1 (ν = 0)	T_1 ($\nu = \langle\nu_{xx}^{PAS}\rangle$)	T_1 ($\nu = \langle\nu_{yy}^{PAS}\rangle$)
220	7.0 (6)	6.0 (3)	7.2 (7)
256	4.9 (4)	4.7 (3)	6.3 (5)
289	2.74 (12)	2.37 (05)	2.82 (13)
320	1.09 (05)	0.93 (03)	1.09 (04)
346	0.59 (04)	0.49 (02)	0.61 (04)

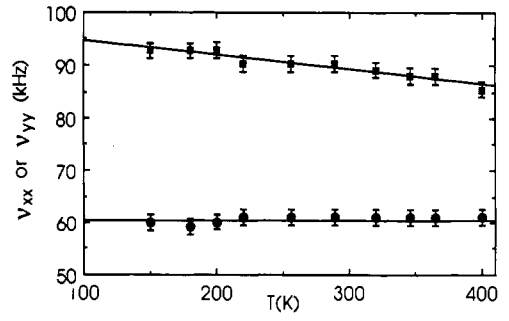

FIGURE 4: Graphs of the poly(γ-benzyl-L-glutamate) amide deuteron efg tensor principal frequencies, $\langle\nu_{xx}^{PAS}\rangle$ and $\langle\nu_{yy}^{PAS}\rangle$, as a function of absolute temperature, T.

PBG at 289 K. The spectrum has e^2qQ/h = 202 (2) kHz, η = 0.19, and $T_1 \approx 2.7$ s as compared to e^2qQ/h = 210 (2) kHz, η = 0.137 (2), and $T_1 > 100$ s for the amide deuterons of NAG or e^2qQ/h = 209 (2) kHz, η = 0.13 (1), and $T_1 \approx 100$ s for L-pyroglutamic acid. PBG T_1 values over the temperature range of 220–346 K are given in Table II for relaxation at three frequencies of the powder patterns, ν = 0, ν_{xx}^{PAS}, and ν_{yy}^{PAS}. Typically, the relaxation times decrease by an order of magnitude as the temperature is increased from 220 to 346 K and show little anisotropy, i.e., the relaxation times determined at the three powder-pattern frequencies differ by no more than 25%. Relaxation at the ν = 0 frequency represents N–D bonds approximately at the magic angle relative to the applied field, whereas the ν_{xx}^{PAS} and ν_{yy}^{PAS} frequencies arise from N–D bonds in the powder sample lying approximately in the plane perpendicular to the field. The spectra have insufficient signal-to-noise ratios to determine T_1 values for the N–D bonds parallel to the applied field, $\nu = \nu_{zz}^{PAS}$.

Plotted in Figure 4 are the magnitudes of ν_{xx}^{PAS} and ν_{yy}^{PAS}, determined directly from the well-defined singularities of the powder patterns, versus temperature. In this work these frequencies can be determined to an accuracy of about ±1 kHz. Within this error limit, the small component is independent of temperature, ν_{xx}^{PAS} = 61 (1) kHz, whereas ν_{yy}^{PAS} decreases by a measurable amount as the temperature is raised from 150 K [ν_{yy}^{PAS} = 92.7 (1) kHz] to 400 K [ν_{yy}^{PAS} = 85.5 (1) kHz]. Within experimental error, ν_{yy}^{PAS} varies linearly with temperature at a rate of −0.027 (5) kHz/K. In the limit of zero temperature ν_{yy}^{PAS} = 97 (1) kHz, from which we calculate, with the temperature-independent value of ν_{xx}^{PAS} = 61 (1) kHz, a static coupling constant of e^2qQ/h = 211 (2) kHz or essentially that observed for the stationary amide deuterons in NAG and L-pyroglutamic acid. Although there is no consistent picture of the coupling tensor asymmetry, the magnitude and temperature dependence of the quadrupole coupling and the reduced relaxation time for the amide deuterons in PBG as compared to NAG and L-pyroglutamic acid indicate two important features. First, the presence of small-amplitude torsional dynamics of the polypeptide backbone structure and second, on the basis of the previously established empirical relations and the simple analogues reported here, the amide deuterons in solid PBG are involved in hydrogen bonding with a deuteron–donor distance in the range of 2.1–2.4 Å.

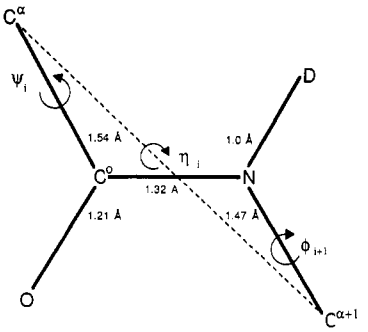

FIGURE 5: Structure of a planar peptide group showing the angles ϕ_{i+1}, ψ_i, and η_i. A change in the angle $\eta_i = \phi_{i+1} - \psi_i$ amounts to a rotation about the axis shown by the dotted line.

That ν_{xx}^{PAS} is temperature independent while the orthogonal components are not indicates reorientation about the ν_{xx}^{PAS} axis, i.e., an axis essentially mutually perpendicular to the peptide plane and the N–D bond. Note that a reorientational process that decreases (averages) ν_{xx}^{PAS} amounts to an unexpected fluctuation of the peptide-bond geometry. A straightforward calculation using standard methods (Wittebort et al., 1987) shows that for a symmetric planar libration the mean-square amplitude, $\langle\theta^2\rangle$, is related to the observed or averaged, $\langle\nu_{ii}^{PAS}\rangle$, and static, ν_{ii}^{PAS}, principal frequencies by

$$\langle\theta^2\rangle = (\nu_{xx}^{PAS} + 2\nu_{yy}^{PAS})^{-1}(\nu_{yy}^{PAS} - \langle\nu_{yy}^{PAS}\rangle) \quad (4)$$

Thus, since $\langle\nu_{yy}^{PAS}\rangle$ is observed to vary linearly with temperature over the range studied (Figure 4), we conclude that the mean-square torsional amplitude, $\langle\theta^2\rangle$, also varies linearly with temperature. Using the linear temperature dependence of $\langle\nu_{yy}^{PAS}\rangle$, ν_{xx}^{PAS} = 61 (1) kHz, and eq 4, we calculate that the mean-square amplitude varies with temperature, T, according to

$$\langle\theta^2\rangle = 1.1\ (2) \times 10^{-4}\ \text{rad}^2K^{-1}T \quad (5)$$

For example, the root-mean-square amplitude, $\theta_{rms} = \langle\theta^2\rangle^{1/2}$, varies from about 8° at 200 K to 12° at 400 K. The linear variation of the mean-square amplitude with temperature suggests harmonic motion, in which case the oscillator frequency is related to the mean-square amplitude by

$$\langle\theta^2\rangle = k_BT/I\omega_T^2 \quad (6)$$

Thus, if the moment of inertia (I) is known, the torsional oscillator frequency (ω_T) is calculated directly from the mean-square amplitude.

Some time ago a simple transformation was proposed (Peticolas & Kurtz, 1980) of the usual peptide backbone conformational angles (ψ_i,ϕ_i) to an alternative set (η_i,ξ_i), which are related by $\eta_i = (\phi_{i+1} - \psi_i)/2$ and $\xi_i = \phi_{i+1} + \psi_i$. The utility of the alternative for the present discussion is that in α-helical polypeptides, the η_i are relatively free to change through modest angles (Peticolas & Kurtz, 1980) and to a very good approximation the corresponding motion, shown in Figure 5, amounts to a reorientation of the peptide plane about the ν_{xx} principal axis of the amide deuteron quadrupole coupling tensor. Thus a fluctuation in η would lead to the type of averaging observed here, and for the sake of argument we assume $\langle\theta^2\rangle = \langle\eta^2\rangle$. With idealized sp^2 peptide-bond angles and standard bond lengths, the moment of inertia (I) for rotation of the atoms in a single peptide group about the axis shown in Figure 5 is immediately calculated, I = 53 gÅ^2/mol. This rotation is not strictly local, i.e., independent for a single peptide group, in that comparatively small rearrangements of neighboring atoms must also occur. The collective nature of

this type of motion has been stressed in theoretical studies (Levitt et al., 1985; Brooks & Karplus, 1983). Thus the moment of inertia calculated in this approximation presumably represents a lower limit that in turn, with eqs 5 and 6, suggests an upper limit for the torsion frequency of $\omega_T \lesssim 63$ cm^{-1}.

We now consider the PBG relaxation data listed in Table II. Since the residual quadrupole coupling has provided an estimate of the mean-square amplitude of the dynamics, the relaxation data are useful for examining dynamic rates and their temperature dependence. In order to proceed, some assumptions about the dynamics must be made. First, since the powder-pattern shapes are clearly dominated by the quadrupolar coupling as opposed to ^{2}H–^{1}H or ^{2}H–^{14}N dipolar coupling, and the T_1 values are two orders of magnitude shorter than for a rigid system, e.g., NAG, we assume spin relaxation results only from torsional reorientation of the quadrupole coupling tensor or equivalently the N–D bond, in which case the general expression for the relaxation time is (Torchia & Szabo, 1982)

$$1/T_1 = (3/16)(e^2qQ/\hbar)^2[J_1(\omega_0) + 4J_2(2\omega_0)] \quad (7)$$

Furthermore, small-amplitude reorientations in solids are generally expected to be quite fast in comparison to the NMR frequency, ~40 MHz here. In the appendix we show that two models for torsional dynamics, (a) an overdamped stochastic process and (b) reorientation described by the Langevin equation for a damped harmonic oscillator, both give the following form for the spectral density

$$J_m = (3/2)\ \langle\theta^2\rangle\tau \quad (8)$$

where τ is the reorientational correlation time and

$$1/\tau \approx D/\langle\theta^2\rangle \quad (9)$$

where D is the diffusion constant.

From the quadrupole coupling for NAG (qcc = 210 kHz) and the temperature-dependent mean-square amplitude (eq 5), we calculate that the correlation times are 2.3 ps at 220 K and increase to 20 ps at 346 K, corresponding to diffusion constants of $D = 12 \times 10^9$ s^{-1} and $D = 1.8 \times 10^9$ s^{-1}, respectively. Thus the temperature dependence of the correlation time is opposite to that normally observed in simple fluids. In other words, the relaxation rate increases with temperature more rapidly than is expected on the basis of the increase in the mean-square librational amplitude. Within the constraints of this model, the usual approach at this point is to assume that the dynamic rate is slow compared to the NMR frequency. With this assumption one calculates that τ shortens from 2.6 μs at 220 K to 0.34 μs at 346 K. However, based on reasonable expectations (McCammon & Harvey, 1987), these dynamic rates are too slow by several orders of magnitude, and we anticipate that correlation times in the picosecond range provide the better qualitative estimate.

In summary, we have accurately determined the molecular orientation of the electric field gradient tensors for the amide and carboxyl deuterons of NAG. The amide deuteron tensor orientation is essentially equivalent to that determined for urea deuterons. We thus expect that the tensor orientation placing the large component along the bond axis and the intermediate component normal to the molecular planes defined above can reasonably be used for a variety of peptide or carboxyl systems. We note that the expected coincidence of the tensor principal component orientations with the molecular geometry occurs within experimental error if the tensor principal component orientations are compared with the neutron structure rather than with the X-ray structure. For example, the N–D bond orientations in NAG from the X-ray (Donohue & Marsh, 1962) and neutron (Mackay, 1975) structures differ by about 7°. Thus accurate determination of the molecular orientation of deuterium electric field gradient tensors probably requires comparison with a structure obtained by neutron diffraction.

The quadrupole couplings for NAG and L-pyroglutamic acid are in satisfactory agreement with empirical relations based on hydrogen-bond lengths. The similarity of these couplings with those obtained from PBG when extrapolated to low temperature indicates that the amide deuterons in solid PBG (obtained by removal of trifluoroacetic acid) are also hydrogen bonded. Certainly side-chain and/or backbone carbonyl oxygens are the donor atoms. PBG when dissolved in weakly hydrogen-bonding solvents such as benzyl alcohol forms intramolecular hydrogen bonds that result in an α-helical structure (Poliks et al., 1987). Strongly hydrogen-bonding solvents such as trifluoroacetic acid break up the helix by forming intermolecular hydrogen bonds. It is interesting to note that simultaneous removal of trifluoroacetic acid and condensation to a solid phase apparently results in α-helix formation (Brumberger & Cheng, 1974) and the restoration of amide hydrogen bonds.

As the temperature of PBG is raised, the components of the electric field gradient tensor along the bond axis and approximately perpendicular to the peptide plane decrease, whereas the mutually orthogonal component remains constant. Thus the N–D bond librates in a plane essentially perpendicular to the peptide plane, and the mean-square amplitude is determined directly from the temperature dependence of the residual coupling.

The presence of small-amplitude motion is also strongly indicated by the much reduced ^{2}H relaxation times relative to NAG or L-pyroglutamic acid. The T_1 value for the amide deuterons in NAG at room temperature is of the order of a hundred seconds, whereas for PBG the T_1 is of the order of a second (220–350 K). It is difficult to anticipate what determines the rather long ^{2}H relaxation times in a highly rigid molecule like crystalline NAG; however, in solid PBG librational reorientation of the quadrupole coupling is expected to be the dominant relaxation process. Whether the dynamics are (a) purely diffusive or (b) a damped Langevin oscillation, the NMR relaxation time in the limit of small amplitude ($\theta_{rms} < 25°$) is determined by the diffusion constant, D, and mean-square amplitude, $\langle\theta^2\rangle$. The essential qualitative point to be made is that the observation of efficient spin relaxation strongly indicates the presence of damping effects that become more prominent as the temperature increases and give the dynamics a diffusive character. In the terms used to describe simple fluids, the Stokes frictional constant is independent of temperature, whereas here the friction increases with temperature. As discussed in the appendix, coherent oscillatory motions are expected to be of sufficiently high frequency to be ineffective in affecting spin relaxation unless the oscillations are damped. The damping constant, λ, is related to the correlation time by $\lambda = \tau\omega_T^2/2$ (obtained by comparing eqs 17 and 22 of the appendix). Using the upper limit for the oscillator frequency of 63 cm^{-1} and the τ values discussed above, one calculates that the oscillations are highly overdamped, i.e., $\lambda/2\pi \sim 8 \times 10^2$ cm^{-1} at 220 K and $\lambda/2\pi \sim 7 \times 10^3$ cm^{-1} at 346 K. Since the calculated damping constants depend quadratically on the oscillator frequency, decreasing the frequency by an order of magnitude from our estimate of an upper limit decreases the calculated damping constants by two orders of magnitude and brings them in the range of 8–70 cm^{-1}, i.e., close to the underdamped regime.

Several other lines of evidence suggest that these qualitative conclusions from the relaxation data are appropriate. First, inelastic neutron-scattering spectra from solid myoglobin (Smith et al., 1989) show a shift in the vibrational density of states to lower frequencies with higher friction and an increase in quasielastic scattering as the temperature is raised. At 300 K the myoglobin spectrum is broadened by frictional damping and dominated by the peak from quasielastic scattering, i.e., diffusive processes with vanishing mode frequency. Second, a recent comparative study by molecular dynamics and normal mode simulations (Perahia et al., 1990) of α-helical decaglycine in vacuo indicates that the harmonic and molecular dynamics descriptions are similar if the force constants or vibrational frequencies used in the normal mode calculation are decreased with increasing temperature. Furthermore, at high temperature (300 K), mode damping is substantially more important than at low temperature (50 K), thus showing an increase of friction with temperature. Finally, normal mode type calculations of small proteins have been extended to include frictional effects by way of a many-body Langevin model (Case & Kottalam, 1990). If a reasonable value for solvent viscosity is used, the calculated correlation functions for low frequency modes (7–18 cm^{-1}) are overdamped and have decay constants in the range of 1–8 ps, i.e., very similar to the correlation times estimated here experimentally.

ACKNOWLEDGMENTS

We thank Professor John Richardson for indexing the NAG crystals by X-ray crystallography.

APPENDIX

The spectral densities, $J_1(\omega_0)$ and $J_2(2\omega_0)$, needed for calculating the longitudinal relaxation rate of eq 7 are determined here for restricted diffusion about an axis and a damped harmonic oscillator in equilibrium with a heat bath. We show that for rapid small-amplitude dynamics, the effect on NMR relaxation for both models is nearly equivalent.

First we solve the geometrical problem common to both models and determine the general form of the correlation function, $C_m(t)$, which is related to the spectral densities by the following Fourier transform:

$$J_m(\omega) = 2\int_0^\infty C_m(t)\cos\omega t\,dt \approx 2\int_0^\infty C_m(t)\,dt \quad (10)$$

For the case at hand we are concerned with motions varying in time rapidly compared to the NMR frequency, and the Fourier transform is well approximated by the integral of the correlation function, resulting in a frequency-independent spectral density. With the reasonable approximation that the quadrupole coupling tensor is axially symmetric, the required correlation function, according to the notation of Torchia and Szabo (1982) and Wittebort and Szabo (1978), is

$$C_m(t) = \sum_{a,a'=-2}^{2} d^{(2)}_{ma}(\beta)d^{(2)}_{ma'}(\beta)e^{-i(a-a')\gamma}C_{aa'}(t) \quad (11)$$

$$C_{aa'}(t) = \langle d^{(2)}_{a0}[\theta(0)]d^{(2)}_{a'0}[\theta(t)]\rangle e^{-i(a-a')\phi} \quad (12)$$

The $d^{(j)}_{k}(\beta)$ are reduced Wigner rotation matrix elements, the angles (θ,ϕ) specify the polar orientation of the unique axis of the efg tensor (essentially the N–D bond) in some frame, and (β,γ) in turn specifies the orientation of that frame with respect to the magnetic field, $\mathbf{H_0}$. If we take $\beta = 90°$ and expand the time-dependent angle θ in a Taylor series about zero, then we have the desired correlation function for the amide deuterons contributing to the perpendicular edge of the powder pattern and undergoing small-amplitude dynamics. Since the amplitudes under consideration are small, $\theta < 20°$, we need only expand $d^{(j)}_{k}(\beta)$ to first order, which gives a second-order correlation function. The nonzero time-dependent terms are

$$C_{\pm1\pm1}(t) = -C_{\mp1\pm1}(t) = (3/2)\langle\theta(0)\theta(t)\rangle \quad (13)$$

Nonzero time-independent terms are dropped since they do not contribute to relaxation. Now, substituting eq 13 into eq 11 with $\beta = 90°$ gives the general form for $C_m(t)$

$$C_m(t) = (3/4)[1 - (-1)^m\cos 2\phi]\langle\theta(0)\theta(t)\rangle \quad \text{with } m = 1, 2 \quad (14)$$

where ϕ is the angle between the plane of the libration and $\mathbf{H_0}$. As a practical matter for powder spectra, all values of ϕ with $\beta = 90°$ will have similar frequencies near the perpendicular edge of the powder pattern and as a useful approximation we average over this angle thus obtaining

$$C_m(t) = (3/4)\langle\theta(0)\theta(t)\rangle \quad (15)$$

The problem is now reduced to determining the single correlation function $\langle\theta(0)\theta(t)\rangle$ for the two models.

For stochastic diffusion about an axis restricted to occur between the limits of $\pm(3\langle\theta^2\rangle)^{1/2}$, one obtains the following correlation function and its spectral density directly from a small-angle expansion of equation 3.12(a–c) of Wittebort and Szabo (1978):

$$\langle\theta(0)\theta(t)\rangle = \langle\theta^2\rangle e^{-t/\tau} \quad (16)$$

$$J_m = (3/2)\langle\theta^2\rangle\tau \quad (17)$$

$$1/\tau \approx \pi^2 D/12\langle\theta^2\rangle \quad (18)$$

where D is the diffusion constant and we have assumed that $1/\tau$ is large compared to the NMR frequency, ω_0. An expression equivalent to eqs 17 and 18 has been used under the assumption of a 2-fold stochastic jump process.

The effect on magnetic relaxation by torsional oscillation of the efg tensor orientation was first considered by Bayer (1951), who used a heuristic quantum-mechanical approach. The basic assumption is that an optical process such as a torsional oscillation ($\omega_T > 1$ cm^{-1}) can cause transitions in a magnetic resonance experiment ($\omega_0 \sim 10^{-2}$ cm^{-1}) by rapid transitions among the quantized torsional states. Woessner and Gutowsky (1963) refined this argument by an improved treatment of the vibrational state lifetimes and gave an explicit calculation of the correlation function $\langle\theta(0)\theta(t)\rangle$. Since we anticipate that an oscillator that results in efficient NMR relaxation must be of low frequency ($\omega_T < k_BT \sim 200$ cm^{-1} at room temperature), a classical approach is used here that more simply relates both the stochastic and mechanical aspects of the oscillatory dynamics to the NMR relaxation times.

Using Chandrasekhar's solution of the Langevin equation for a damped harmonic oscillator in equilibrium with a heat bath (Chandrasekhar, 1943), Szabo (1984) obtained the correlation function

$$\langle e^{ia\theta(0)}e^{-ia'\theta(t)}\rangle = \exp\left\{-\frac{1}{2}\langle\theta^2\rangle\left[a^2 + a'^2 - 2aa'e^{-\lambda t}\left(\cosh\mu t + \frac{\lambda}{\mu}\sinh\mu t\right)\right]\right\} \quad (19)$$

where $\mu = (\lambda^2 - \omega_T^2)^{1/2}$ and the damping constant $\lambda = \zeta/2I$ in which ζ is the Stokes friction constant. The friction constant can be related to a diffusion constant by the Einstein relation, $D = k_BT/\zeta$. Even though the system is damped, the oscillator frequency, ω_T, is related to the mean-square amplitude and

moment of inertia, I, by the classical equipartition relation in eq 6 (Chandrasekhar, 1943). The desired second-order correlation function is obtained as a small-angle approximation of eq 19 by expanding the exponentials on the left-hand side to first order in $\theta(0)$ and $\theta(t)$ and that on the right-hand side to first order in $\langle\theta^2\rangle$. The result is

$$\langle\theta(0)\theta(t)\rangle = \langle\theta^2\rangle e^{-\lambda t}\left(\cosh \mu t + \frac{\lambda}{\mu}\sinh \mu t\right) \quad (20)$$

which can be compared directly with the purely diffusive model in eq 16. Note that for an underdamped oscillator, $\omega_T > \lambda$, μ is imaginary, and the correlation function has a coherent oscillation. In the limit of weak damping, eq 20 decays with a time constant of $1/\lambda$, whereas in the limit of strong damping the time constant is $\langle\theta^2\rangle/D$ and eq 20 is nearly equivalent to eq 16. The fast-limit spectral density is

$$J_m = 3\langle\theta^2\rangle(\lambda/\omega_T^2) \quad (21)$$

It is interesting to note that eq 21 is equivalent to the result of Woessner and Gutowsky (1963) in the limit of high temperature if the reciprocal of the classical damping constant is equated to their definition of an average lifetime for a vibrational state. Whereas eq 17 results from a Lorentzian spectral density centered at zero frequency, eq 21 comes from a spectral density centered at the oscillator frequency and has the expected features that J_m or the relaxation rate is inversely proportional to the square of the oscillator frequency and proportional to the damping constant. In the limit of no oscillator damping (large diffusion constant or small friction constant), the spectrum is a δ function centered at ω_T, which is widely separated from the NMR frequency and thus induces no NMR transitions. The damped oscillator result, eq 21, is more readily compared to both the observed experimental results of this paper and the diffusion-only result, eq 17, by using eq 6 and the definitions of D and λ. The result is equivalent to the diffusion expression for J_m, eq 17, with a slightly different correlation time.

$$1/\tau = D/\langle\theta^2\rangle \quad (22)$$

Thus, in the limit of rapid, small-angle, and damped oscillations, the effect of the restoring force on the NMR relaxation is accounted for in terms of its effect on the mean-square amplitude; a feature that is included by assumption in the restricted diffusion model.

References

Arfken, G. (1971) *Mathematical Methods for Physicists*, 2nd ed., pp 178–180, Academic Press, New York.

Bayer, H. (1951) *Z. Phys. 130*, 227–238.

Brooks, B., & Karplus, M. (1983) *Proc. Natl. Acad. Sci. U.S.A. 80*, 6571–6575.

Brumberger, H., & Cheng, B. (1974) *Biopolymers 13*, 2653–2656.

Case, D. A., & Kottalam, J. (1990) *Biopolymers 29*, 1409–1421.

Chandresekhar, S. (1943) *Rev. Mod. Phys. 15*, 1–89.

Chapman, G. E., Campbell, I. D., & McLauchlan, K. A. (1970) *Nature 225*, 639–641.

Chiba, T. (1965) *Bull. Chem. Soc. Jpn. 38*, 259–263.

Donohue, J., & Marsh, R. E. (1962) *Acta Crystallogr. 15*, 941–946.

Hunt, M. J., & Mackay, A. L. (1976) *J. Magn. Reson. 22*, 295–301.

Levitt, M., Sander, C., & Stern, P. S. (1985) *J. Mol. Biol. 181*, 423–447.

Looyestijn, W. J., Klaassen, T. O., & Poulis, N. J. (1979) *Physica B96*, 303–311.

Mackay, M. F. (1975) *Cryst. Struct. Commun. 4*, 225–228.

McCammon, J. A., & Harvey, S. C. (1987) *Dynamics of Proteins and Nucleic Acids*, pp 25–34, Cambridge University Press, Cambridge.

Perahia, D., Levy, R. M., & Karplus, M. (1990) *Biopolymers 29*, 645–677.

Peticolas, W. L., & Kurtz, B. (1980) *Biopolymers 19*, 1153–1166.

Poliks, M. D., Park, Y. W., & Samulski, E. T. (1987) *Mol. Cryst. Liq. Cryst. 153*, 321–346.

Press, W. H., Flannery, B. P., Teukolsky, S. A., & Vetterling, W. A. (1986) *Numerical Recipes*, pp 523–529, Cambridge University Press, Cambridge.

Smith, J., Kuczera, K., Tidor, B., Doster, W., Cusack, S., & Karplus, M. (1989) *Physica B 156 & 157*, 437–443.

Szabo, A. (1984) *J. Chem. Phys. 81*, 150–167.

Torchia, D. A., & Szabo, A. (1982) *J. Magn. Reson. 49*, 107–121.

Tycko, R., Schneider, E., & Pines, A. (1984) *J. Chem. Phys. 81*, 680–688.

Usha, M. G., & Wittebort, R. J. (1989) *J. Mol. Biol. 208*, 669–678.

Van Zoeren, E., Oonk, H. A. J., & Kroon, J. (1978) *Acta Crystallogr. B34*, 1898–1900.

Witterbort, R. J., & Szabo, A. (1978) *J. Chem. Phys. 69*, 1722–1736.

Wittebort, R. J., Woehler, S. E., & Bradley, C. H. (1986) *J. Magn. Reson. 67*, 143–145.

Wittebort, R. J., Olejniczak, E. T., & Griffin, R. G. (1987) *J. Chem. Phys. 86*, 5411–5420.

Woessner, D. E., & Gutowsky, H. S. (1963) *J. Chem. Phys. 39*, 440–456.